CONF-911111--18

DE92 005121

THE EFFECT OF NEUTRON IRRADIATION ON THE STRUCTURE AND PROPERTIES OF CARBON-CARBON COMPOSITE MATERIALS*

T. D. Burchell, W. P. Eatherly, J M Robbins, and J. P. Strizak

ABSTRACT

Carbon-based materials are an attractive choice for fusion reactor plasma facing components (PFCs) because of their low atomic number, superior thermal shock resistance, and low neutron activation. Next generation plasma fusion reactors, such as the International Thermonuclear Experimental Reactor (ITER), will require advanced carbon-carbon composite materials possessing extremely high thermal conductivity to manage the anticipated severe heat loads. Moreover, ignition machines such as ITER will produce high neutron fluxes. Consequently, the influence of neutron damage on the structure and properties of carbon-carbon composite materials must be evaluated.

Data from an irradiation experiment are reported and discussed here. Fusion relevant graphite and carbon-carbon composites were irradiated in a target capsule in the High Flux Isotope Reactor (HFIR) at Oak Ridge National Laboratory (ORNL). A peak damage dose of 1.58 dpa (displacements per atom) at 600°C was attained. The carbon materials irradiated included nuclear graphite grade H-451 and one-, two-, and three-directional carbon-carbon composite materials.

Dimensional changes, thermal conductivity (room temperature), and strength are reported for the materials examined. The influence of fiber type, architecture, and heat treatment temperature on properties and irradiation behavior are reported. Carbon-carbon composite dimensional changes are interpreted in terms of simple microstructural models.

1. INTRODUCTION

Carbon- and graphite-based materials are used extensively in experimental fusion energy reactors for plasma facing applications. Existing large devices such as the Tokamak Fusion Test Reactor (TFTR), the Japan Atomic Energy Research Institutes JT60U, and General Atomics DIIID utilize carbon-carbon composite plasma facing materials in their limiters and/or diverters. Carbon-based materials are an attractive choice for plasma interactive component armor because of their low atomic number, high-thermal shock resistance, and lack of a melting temperature (graphite sublimes at ~3600 K). Fusion reactors such as the International Thermonuclear Experimental Reactor (ITER) have selected carbon materials as the design-basis first wall armor and diverter materials. Plasma facing components in ITER must endure a severe environment, including very high heat fluxes during plasma collapse, and irradiation damage arising from impinging 14.1 MeV fusion neutrons. Consequently, the effect of neutron damage on the structure and properties of carbon-carbon composite materials must be elucidated.

---

*Research sponsored by the Office of Fusion Energy, U.S. Department of Energy, under Contract DE-AC05-84OR21400 with Martin Marietta Energy Systems, Inc.

The manufacture of carbon-carbon composites[1] involves two distinct processes, i.e., preform weaving and component densification. The preform can be woven from polyacrylonitrile (PAN), rayon, or pitch based fibers. The preparation, structure, treatment, and properties of carbon fibers are reported extensively elsewhere.[2] The dry-woven preform is converted to a densified composite by repetitive pitch impregnation or carbon vapor infiltration, followed by carbonization, typically at 700-1000°C, and then graphitization (at a temperature above 2400°C). The preform is reimpregnated, carbonized, and graphitized several times in order to increase the density to as much as 2.0 g/cm^3.

The influence of neutron irradiation on the structure and properties of graphite has been extensively studied.[3-6] More recently, the effects of radiation damage on GraphNOL N3M, a candidate fine-grained graphite for fusion reactor first wall applications, have been reported.[7] Neutron irradiation causes the displacement of carbon atoms from their equilibrium lattice positions into interstitial locations, leaving vacancies in the basal planes. Interstitial carbon atoms become increasingly mobile at higher temperatures, forming clusters and eventually new planes (Fig. 1).

A consequence of this damage is a rapid increase in the graphite's strength and modulus. Kelly[8] has attributed these increases to the pinning of basal plane dislocations by irradiation induced defects. Subsequent changes in the graphite's strength and modulus occur due to changes in the polycrystalline structure of the graphite, which also affects the volume. Initially there is volume shrinkage, but the shrinkage rate decreases, and reversal to growth occurs at higher fluence. As the irradiation temperature increases, the effect is accelerated and shrinkage reversal occurs at lower neutron fluence.

In contrast, very little work has been performed to determine the effects of neutron irradiation on carbon-carbon composites.[9,10] Gray[11] and Price et al.,[12] have reported data on the irradiation induced dimensional changes of carbon fibers. The fibers were observed to shrink along their length while the fiber diameter initially shrunk and subsequently reversed and swelled. This type of behavior has been interpreted in terms of microstructural models and graphite single crystal behavior.[13] Essentially, the fiber crystallographic structure is modelled as a core-sheath arrangement (Fig. 2), with the c-direction radially and the two a-directions aligned axially and circumferentially. From single crystal behavior a-axis shrinkage and c-axis growth is expected to occur. However, just as in the case of bulk graphites, the c-axis growth is initially accommodated by "interplaner" voidage. Therefore, macroscopically fiber axial shrinkage and fiber diametral shrinkage occur followed by swelling (due to c-axis growth). Burchell et al[13] have reported that two-directional carbon-carbon composite specimens exhibited an increase in thickness (perpendicular to the fabric layers) and a shrinkage in diameter (parallel to the fiber axis) on irradiation at 400°C to approximately 12 dpa. The irradiation behavior of uni-directional (1D), two-directional (2D), and three-directional (3D) carbon-carbon composites are reported herein.

2. EXPERIMENTAL

Irradiations were performed in the target region of the High Flux Isotope Reactor (HFIR) at the Oak Ridge National Laboratory (ORNL). The irradiation capsule design, designated HTFC1, was neon-gas filled, and the specimen temperature was controlled by sizing the annular gap between the specimen and capsule. Silicon carbide temperature monitors were placed at intervals throughout the capsule. The specimens were either hollow cylinders 6.35-mm long, with an ID of 3.2 mm and an OD of 12 mm, or solid cylinders of 12-mm diameter with lengths ranging from 6 to 12 mm. A maximum fluence of 2.44×10^{25} n/m^2 [E > 50 KeV] or ~.6 dpa was attained at an irradiation temperature of 600°C.

The materials used here are summarized in Table 1. Two heat treatment temperatures were employed for the three-directional carbon-carbon composite materials, i.e., 2650°C and 3100°C. Heat treatment was conducted in a graphite resistance furnace under an inert atmosphere. Pre-irradiation characterization included dimensional measurement and specimen mass. Thermal diffusivity and brittle ring strength were measured on unirradiated control specimens cut from adjacent locations in the carbon-carbon composite billets. The room temperature thermal conductivity was calculated from the room temperature diffusivity, measured by the thermal-pulse technique, using the formula

$$K = \alpha \rho C_v \ (W/m \cdot K).$$

Where α is the thermal diffusivity (m^2/s), ρ is the specimen density (kg/m^3) and C_v is the specific heat at constant volume ($J/kg \cdot K$). The brittle ring strength was calculated using the formula

$$S = \frac{6 \cdot K_t \cdot P \cdot (D_2 + D_1)}{\pi \cdot h \cdot (D_2 - D_1)^2} (MPa).$$

Where K_t is the stress intensity factor, equal to 1.25 (m^{-1}) for the ring geometry used here. P is the load at failure (N), D_2 is the outside diameter (m), D_1 is the inside diameter (m) and h is the ring thickness (m).

Table 1. Summary of materials in HFIR capsule HTFC1

Designation	Description	Heat Treatment Condition
H-451	Near-isotropic nuclear graphite (reference material).	As received
A05	Carbone Lorraine. Two-directional carbon-carbon composite. PAN Fibers.	As received
UFC	Fiber Materials, Inc. Uni-directional fiber composite. PAN Fibers.	3100°C
RFC	Fiber Materials, Inc. Random fiber composite. PAN Fibers (chopped).	As received
223	Fiber materials, Inc. Three-directional fiber composite. PAN Fibers.	2650 and 3100°C
222	Fiber Materials, Inc. Three-directional fiber composite. Pitch Fibers (P55).	2650 and 3100°C

3. RESULTS AND DISCUSSION

3.1 DIMENSIONAL CHANGE

Irradiation induced dimensional and volume change data are reported and discussed below in terms of (i) architecture, i.e., uni-directional, two-directional, or random fiber orientation; (ii) fiber

precursor, i.e., pitch versus PAN (texture and crystallinity); and (iii) effect of heat treatment temperature (crystallinity).

3.1.1 The Influence of Architecture

Figures 3 and 4 summarize the data for H-451, A05, RFC, and UFC materials in the preferred <a> and preferred <c> directions, respectively. For the composite materials (RFC, UFC, and A05) these translate to: (i) parallel to the fiber axis for the preferred <a> direction and (ii) perpendicular to the fiber axis for the preferred <c> direction. For the bulk graphite, H-451, these translate to (i) parallel to the extrusion direction for the preferred <a> direction, and (ii) perpendicular to the extrusion direction for preferred <c> direction.

The observed irradiation induced shrinkage of the reference graphite, grade H-451, was as expected. The greater observed shrinkage in the preferred <a> direction compared with that in the preferred <c> direction is attributed to the texture and near-isotropic nature of grade H-451. Such behavior is well known,[3-6] and has recently been reported for PGA, an extruded nuclear grade graphite.[14] Similarly, the random fiber composite material shrank in a near-isotropic manner.

In contrast to H-451 and RFC, the uni-directional (UFC) and two-directional (A05) carbon-carbon composites exhibit very marked anisotropy in their shrinkage. Indeed, for A05 the preferred <a> direction shrinkage is in excess of four times the preferred <c> shrinkage. Moreover, UFC exhibits five to ten times more shrinkage in the preferred <a> direction than in the preferred <c> direction.

The irradiation induced dimensional changes of the carbon-carbon composite materials can best be understood in terms of the fiber microstructure and composite architecture. Several models of carbon fiber structure have been proposed. Recently, many of these models were reviewed by Donnet and Bansal.[2] A simple model of fiber microstructure, which may be used to interpret the irradiation data, is shown in Fig. 2. At the relatively low fluences considered here, the fiber behavior will be dominated by shrinkage in the <a> direction, resulting in both axial and diametral shrinkages. Swelling in the <c> direction may be initially accommodated by the interplaner voids and pores, or, is perhaps accommodated by the extensive network of cracks known to exist within the carbon-carbon composite, such as those within fiber bundles, or at fiber bundle matrix interfaces.[15] Therefore, the behavior of the composite materials is dominated by fiber axial shrinkage (preferred <a> direction), as clearly shown in Fig. 3 for the UFC and A05 materials. The random dispersion of chopped fibers in RFC imparts a high degree of isotropy in its irradiation induced shrinkage. Irradiation induced volume changes for UFC, RFC, A05, and H-451 are shown in Fig. 5. All of the carbon-carbon composite materials exhibit more volume contractions than H-451 graphite.

3.1.2 The Influence of Fiber Precursor

The influence of fiber precursor was examined by comparing two three-directional carbon composites, one manufactured from a pitch precursor fiber (222), and the other manufactured from a PAN precursor fiber (223). These data are shown in Figs. 6 and 7, where $\Delta d/d_o$ is the specimen diametral dimensional change and $\Delta h/h_o$ is the height shrinkage, respectively. Clearly the pitch fiber composite (222) exhibits less shrinkage than does the PAN fiber campsite (223). This is attributed to the higher degree of graphitization (crystallinity) of the pitch fibers. A comparison of the PAN composite (223) diametral and height shrinkage shows the material to be very isotropic in irradiation response. In contrast, the pitch fiber composite (222) behavior is less isotropic, the height shrinkage being greater than that in the diametral direction. These differences are probably attributable to

differences in the detailed architecture of the two composites, e.g., fiber tow size; relative distributions in the x, y, and z directions; the fiber bundle spacings; and the total composite fiber content. The difference between irradiation response of the pitch and PAN composites is particularly evident in Fig. 8, which shows the volume changes for H-451, 222, and 223 materials.

3.1.3 The Influence of Heat Treatment

Figures 6, 7, and 8 additionally show the pitch composite (222) and PAN composite (223) at two heat treatment temperatures. The influence of final heat treatment temperature on irradiation response is most readily appreciated from Figs. 6 ($\Delta d/d_o$) and 8 ($\Delta V/V_o$). For the pitch and PAN carbon-carbon composite materials a higher final heat treatment temperature (3100 cf. 2650°C) reduces the total amount of shrinkage for a given fluence. This improved irradiation stability is attributed to increases in the degree of graphitization, or crystallinity, associated with the higher heat treatment temperature.

3.2 STRENGTH MEASUREMENTS

The unirradiated and irradiated strength data for H-451, RFC, 222, and 223 are given in Table 2. When irradiated, the H-451 graphite exhibited a 32% increase in strength. Similarly, the RFC composite with chopped PAN fibers showed a 36% increase in strength when irradiated, however this composite structure appeared to be somewhat weaker than the H-451 graphite.

Table 2. Brittle ring strength data for unirradiated and irradiated carbon-carbon composites and H-451 graphite

Designation	Condition	Fracture Strength (MPa)[a]	Fractional change in strength (σ/σ_o)
H-451	Unirradiated Irradiated	47.8 ± 2.8 (12) 62.9 (1)	1.32
RFC	Unirradiated Irradiated	30.8 ± 2.9 (3) 41.9 (1)	1.36
222 (2650°C)	Unirradiated Irradiated	59.7 ± 12.0 (5) 82.9 ± 4.9 (2)	1.39
222 (3100°C)	Unirradiated Irradiated	49.3 ± 0.5 (3) 65.7 (1)	1.33
223 (2650°C)	Unirradiated Irradiated	90.9 ± 15.8 (5) 160.9 (1)	1.77
223 (3100°C)	Unirradiated Irradiated	89.6 ± 9.6 (5) 131.1 (1)	1.46

[a]Unirradiated data are mean ± one standard deviation, the numbers of tests are in parenthesis.

Two heat treatment temperature conditions were examined for the two three-directional carbon composites. Generally, both the 222 and 223 composite structures were stronger than the H-451 graphite. Heat treatment of the 222 composite at 3100°C resulted in an approximately 20% reduction in strength compared to the 2650°C heat treatment for both unirradiated and irradiated

conditions. Similar to the H-451 graphite, irradiation of the 222 composite resulted in an approximately 35% increase in strength regardless of heat treatment temperature.

The unirradiated 223 composite, the stronger of the three-directional composites, appeared to be unaffected by heat treatment temperature. However, the higher heat treatment temperature resulted in an approximately 20% decrease in strength for the irradiated material. Compared with the 222 composite, irradiation of the 223 resulted in significantly higher increases in strength particularly for material heat treated at 2650°C.

3.3 THERMAL CONDUCTIVITY

The fractional changes in thermal conductivity for UFC (3100°C), A05, 223 (3100°C), and 222 (3100°C) over the fluence range examined here are shown in Fig. 9. The unirradiated room temperature thermal conductivity of UFC (3100°C), A05, 223 (3100°C), and 222 (3100°C) were 239, 136, 159, and 218 W/m•K, respectively. The highest conductivities were for UFC and 222. In the case of UFC, this is attributed to the high fiber fraction in the direction of measurement. The 222 material has a high thermal conductivity because it is made from high modulus (highly crystalline) pitch fibers. The high degree of crystalline perfection minimizes the number of defect related phonon scattering sites, thus yielding a relatively large phonon man free path and high thermal conductivity.

Neutron irradiation is known to degrade the thermal conductivity of graphites[16] and recently the reduction of thermal conductivity of neutron irradiated carbon-carbon composite CX-2002U, a two-direction felt-type material, was reported by Maruyama.[17]

The large reductions in room temperature thermal conductivity shown in Fig. 9 are in agreement with Maruyama's data which showed a fractional thermal conductivity for CX-2002U of approximately 0.1 after irradiation at 400°C to 7.4×10^{24} n/m^2. The irradiation induced reduction in thermal conductivity results from an increase in the defect concentration, i.e., the formation of interstitials and vacancies, which scatter phonons and reduce the mean free path. The lowest fractional conductivity reported here was for composite 222 (3100°C), which reduced from its unirradiated value of 218 w/m·K to 40 W/m·K after 1.46 dpa irradiation at 600°C. Thermal conductivities of composites 223 (3100°C), A05, and UFC (3100°C) were reduced to 36, 32, and 67 W/m·K, respectively, after irradiation under similar conditions. The irradiation induced reduction in thermal conductivity is of major concern for the application of carbon-carbon composites as plasma facing materials. However, thermal annealing of the irradiation damage resulting from elevated operating temperature of the wall-armor material will partly mitigate the loss of conductivity. Typically, the thermal conductivity would be expected to return to better than 50% of the unirradiated value (at the measurement temperature) when measured at >1000°C (i.e., in situ annealing).

4.0 CONCLUSIONS

A series of carbon-carbon composite materials have been irradiated in the HFIR reactor at 600°C to a peak damage dose of 1.6 dpa. Dimensional and volume change data for the composite material studied here have been analyzed in terms of their architecture, reinforcing fiber precursor, and final graphitization temperature.

The dimensional change behavior has been interpreted through a fiber microstructural model and the expected graphite single crystal dimensional changes. These data indicate that 3D materials behave more isotopically than 2D or uni-directional materials. Pitch fiber composites are more

dimensionally stable than PAN fiber composites and a high final heat treatment temperature is beneficial. Thus, an optimum carbon-carbon composite material for maximum dimensional stability would have multi-directional reinforcements (i.e., at least three-directional), small cell size, high-crystallinity pitch fibers, and a high final graphitization temperature.

The effect of neutron damage on strength has been determined by measuring the brittle ring strength of the specimens. The material's behavior was as expected from previous work on graphites, i.e., the strength increases with increasing neutron damage dose. Thermal conductivity was found to reduce markedly on irradiation, the room temperature conductivity typically being less than 30% of the unirradiated value after irradiation at 600°C to 1.6 dpa. The UFC and 222 carbon-carbon composites exhibited the highest room temperature thermal conductivities in the unirradiated condition.

Irradiation induced dimensional and property changes of carbon-carbon composite materials are controlled by such features as architecture, fiber and impregnant type, and processing history. Consequently, differing carbon-carbon composites can not be expected to have similar irradiation behaviors.

5.0 REFERENCES

1. R. B. Dinwiddie, T. D. Burchell, and C. F. Baker, in: Ext. Abs. and Program, 20th Biennial Conference on Carbon, June 23-28, 1991 (American Carbon Society, Santa Barbara, Calif., USA, 1991) p. 642.

2. J. B. Donnet and R. C. Bansal, Carbon Fibers, Second Edition, Pub. Marcel Dekker, Inc., 1990.

3. W. N. Reynolds, in: Chemistry and Physics of Carbon, Vol. 2, Ed. P. L. Walker, Jr. (Marcel Dekker, New York, 1966) p. 121.

4. J. W. H. Simmons, Radiation Damage in Graphite (Pergamon Press, Oxford, 1965).

5. P. A. Thrower, in: Chemistry and Physics of Carbon, Vol. 5, Ed. P. L. Walker, Jr. (Marcel Dekker, New York, 1969) p. 217.

6. G. B. Engle and W. P. Eatherly, High Temp.-High Press., 4 (1972) 119.

7. T. D. Burchell and W. P. Eatherly, in: Journal of Nuclear Materials 179-181 (1991) p. 205.

8. B. T. Kelly, Physics of Graphite (Applied Science Publishers, London, 1981).

9. I. D. Peggs and R. W. Mills, in: Proceedings of 10th Annual Conference on Carbon (American Carbon Society, 1971) p. 188.

10. B. F. Jones, ibid, p. 190.

11. W. J. Gray, BNWL-2390, Battelle Pacific Northwest Laboratories, Richland, Washington, 1970.

12. R. J. Price, R. J. Hopkins, and G. B. Engle, in: Proceedings of 17th Biennial Conference on Carbon (American Carbon Society, 1985) p. 340.

13. T. D. Burchell, W. P. Eatherly, G. W. Hollenberg, O. D. Slagle, and R. D. Watson, in: Ext. Abs. and Program, 20th Biennial Conference on Carbon, June 23-28, 1991 (American Carbon Society, Santa Barbara, Calif., USA, 1991) p. 598.

14. T. D. Burchell and A. J. Wickham, in: Ext. Abs. and Prog. 18th Biennial Conference on Carbon, July 19-24, 1987 (American Carbon Society, 1987) p. 245.

15. T. J. Mays and B. McEnaney, ibid, p. 438.

16. B. T. Kelly, The Thermal Conductivity of Graphite, in: Chem. and Phys. of Carbon, Vol. 5, (Marcel Dekker, New York, 1969) p. 119.

17. T. Maruyama, Changes in the Thermal Properties of Graphite by Neutron Irradiation, in: Proc. of Japan-US Workshop P-165, Critical Topics of PMI/PFC Data for the Next Step Fusion Devices, December 3-6, 1990, National Institute for Fusion Science, Nagoya, Japan

FIGURE CAPTIONS

1. Graphite single crystal structure and irradiation induced dimensional changes.

2. Carbon fiber structural model and orientation of basal planes.

3. The effect of carbon-carbon composite architecture on irradiation induced specimen shrinkage in the preferred <a> direction.

4. The effect of carbon-carbon composite architecture on irradiation induced specimen shrinkage in the preferred <c> direction.

5. The effect of carbon-carbon composite architecture on irradiation induced specimen volume shrinkage.

6. The effect of fiber crystallinity on the irradiation induced diameter shrinkage of 3D carbon-carbon composites.

7. The effect of fiber crystallinity on the irradiation induced height shrinkage of 3D carbon-carbon composites.

8. The effect of fiber crystallinity on the irradiation induced volume shrinkage of 3D carbon-carbon composites.

9. Neutron irradiation induced reduction of room temperature thermal conductivity for carbon-carbon composites.

ORNL-DWG 91-16366

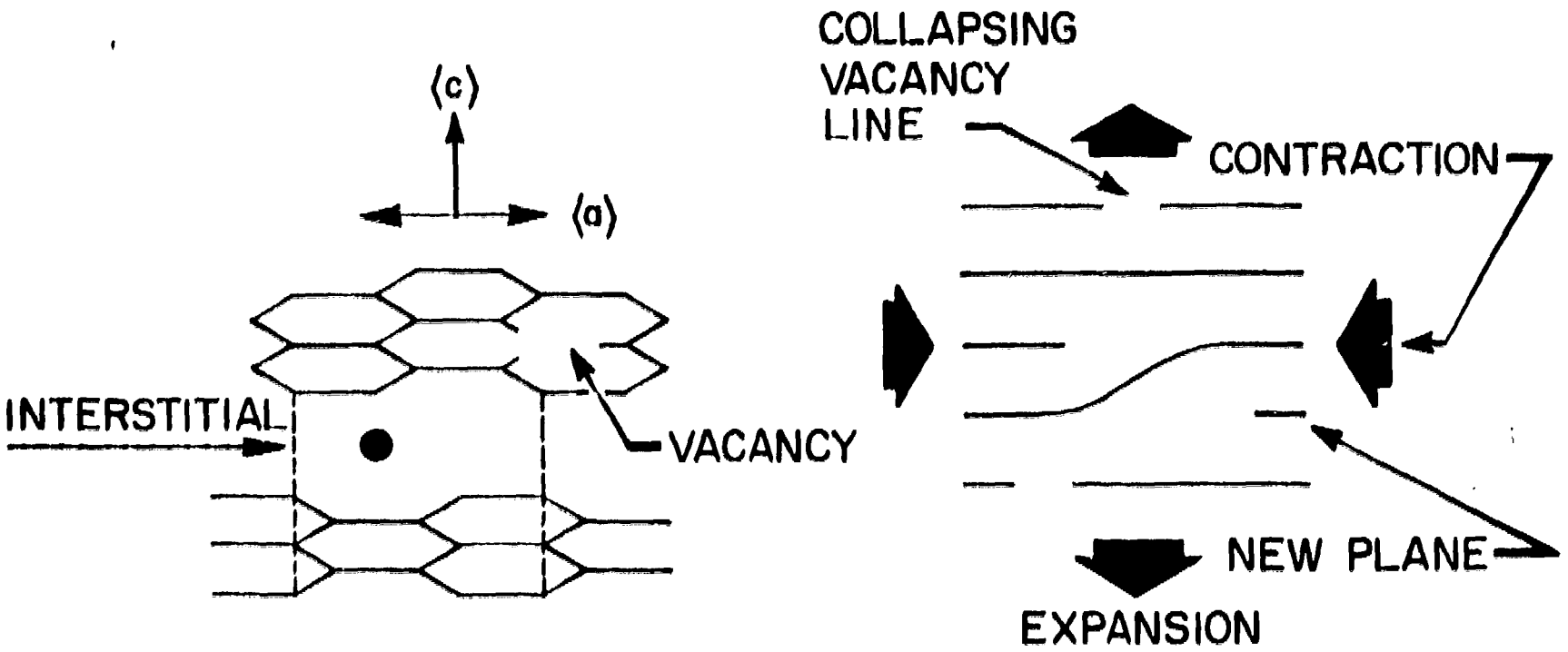

Fig. 1

ornl

ORNL-DWG 91-11079AR

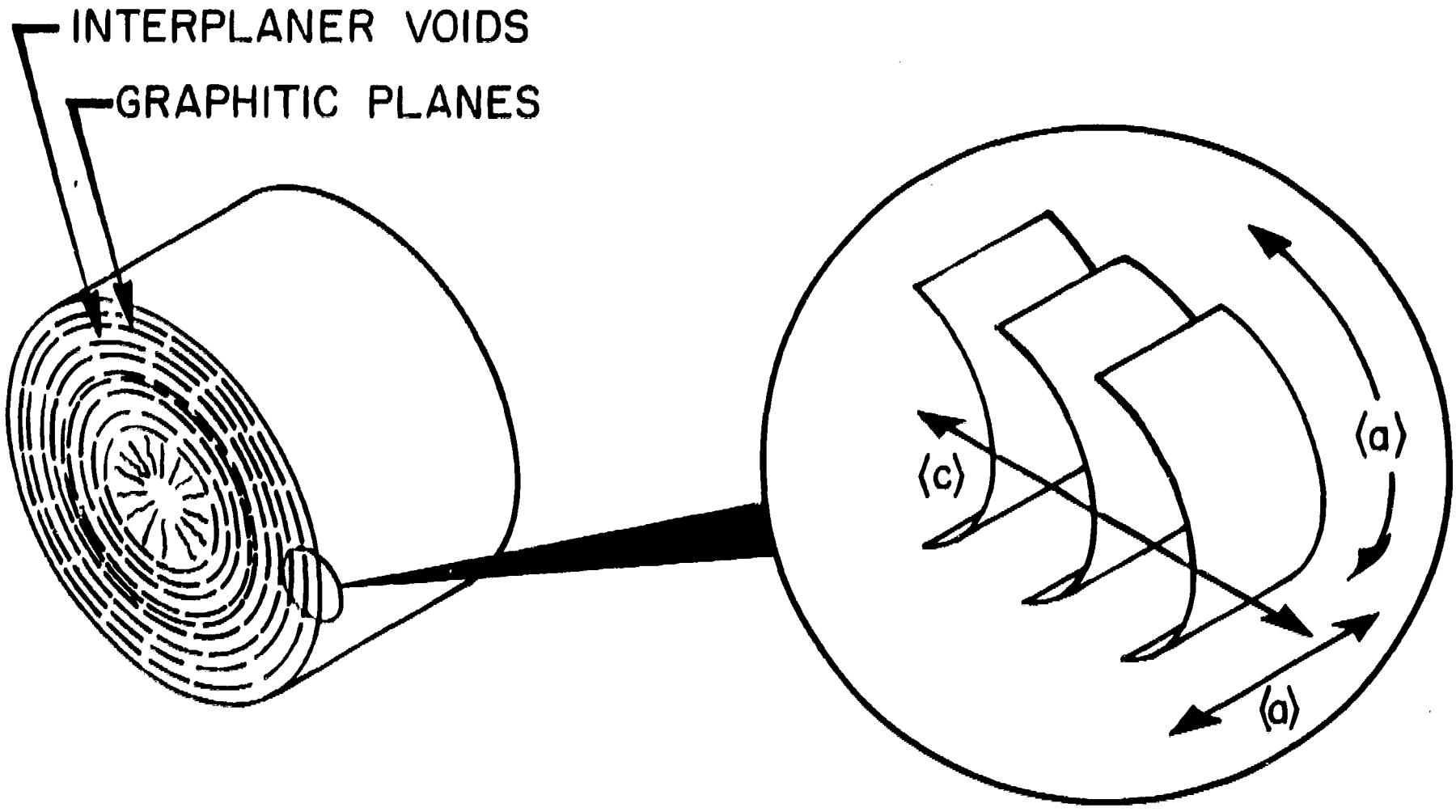

CORE-SHEATH MODEL

Fig. 2

ornl

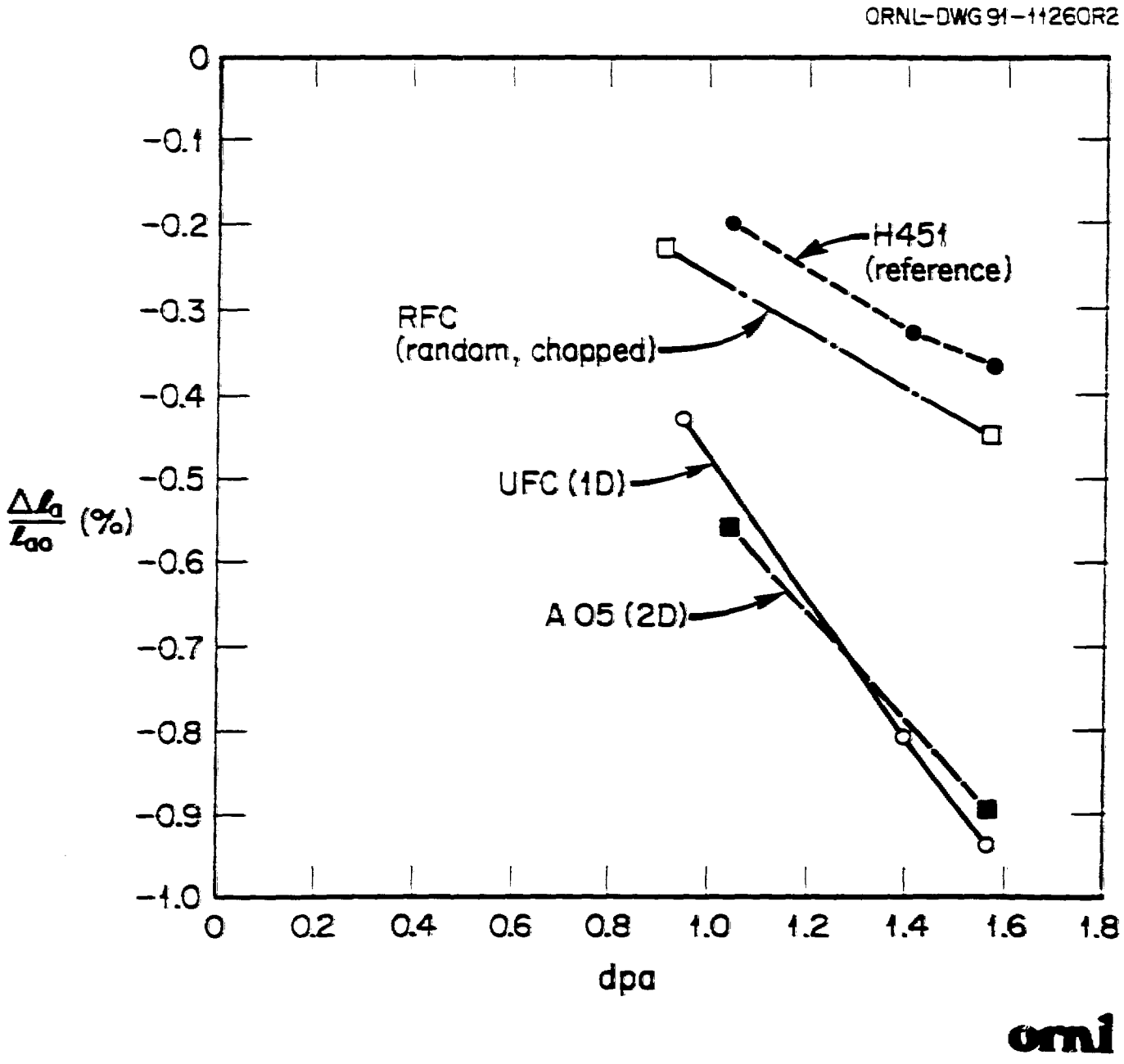
ORNL-DWG 91-11260R2
0
-0.1
-0.2
-0.3
-0.4
-0.5
-0.6
-0.7
-0.8
-0.9
-1.0
$\frac{\Delta \ell_a}{\ell_{ao}}$ (%)
H451
(reference)
RFC
(random, chopped)
UFC (1D)
A 05 (2D)
0
0.2
0.4
0.6
0.8
1.0
1.2
1.4
1.6
1.8
dpa
ornl

Fig. 3

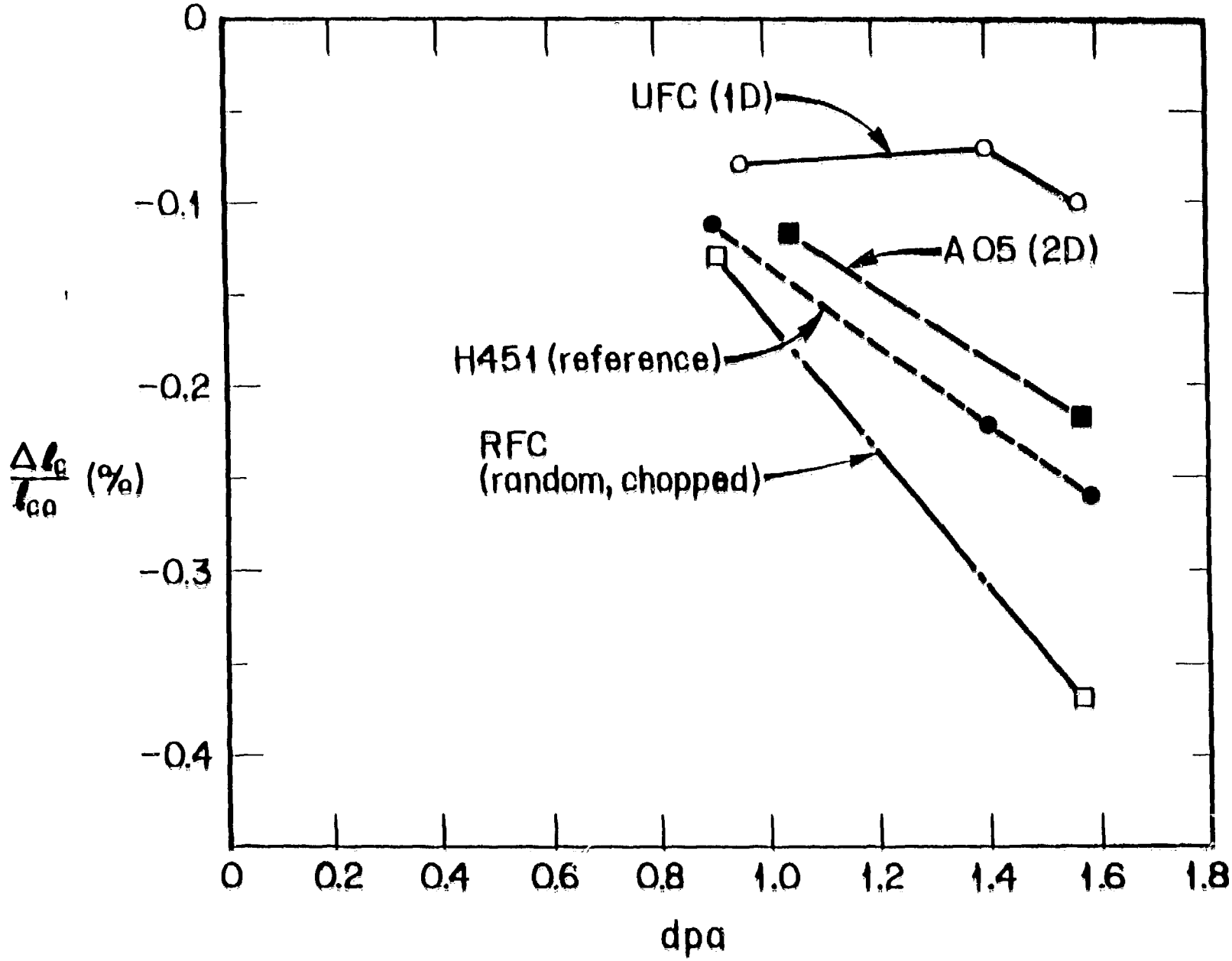
0
-0.1
-0.2
-0.3
-0.4
$\frac{\Delta l_c}{l_{co}}$ (%)
UFC (1D)
A 05 (2D)
H451 (reference)
RFC
(random, chopped)
0
0.2
0.4
0.6
0.8
1.0
1.2
1.4
1.6
1.8
dpa
ornl

Fig. 4

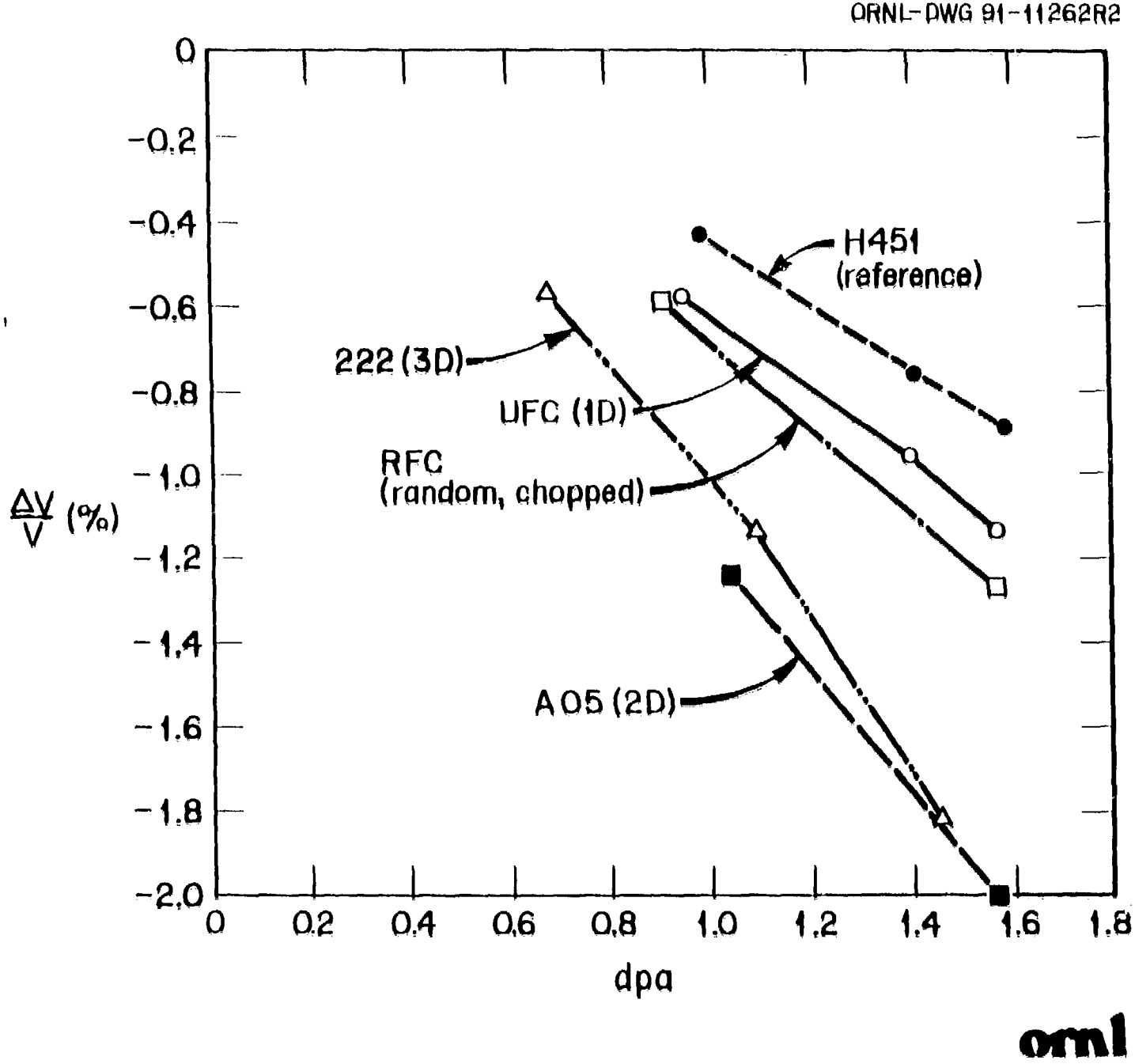
ORNL-DWG 91-11262R2
0
-0.2
-0.4
-0.6
-0.8
-1.0
-1.2
-1.4
-1.6
-1.8
-2.0
ΔV/V (%)
0
0.2
0.4
0.6
0.8
1.0
1.2
1.4
1.6
1.8
dpa
H451
(reference)
222 (3D)
UFC (1D)
RFC
(random, chopped)
A05 (2D)
ornl

Fig. 5

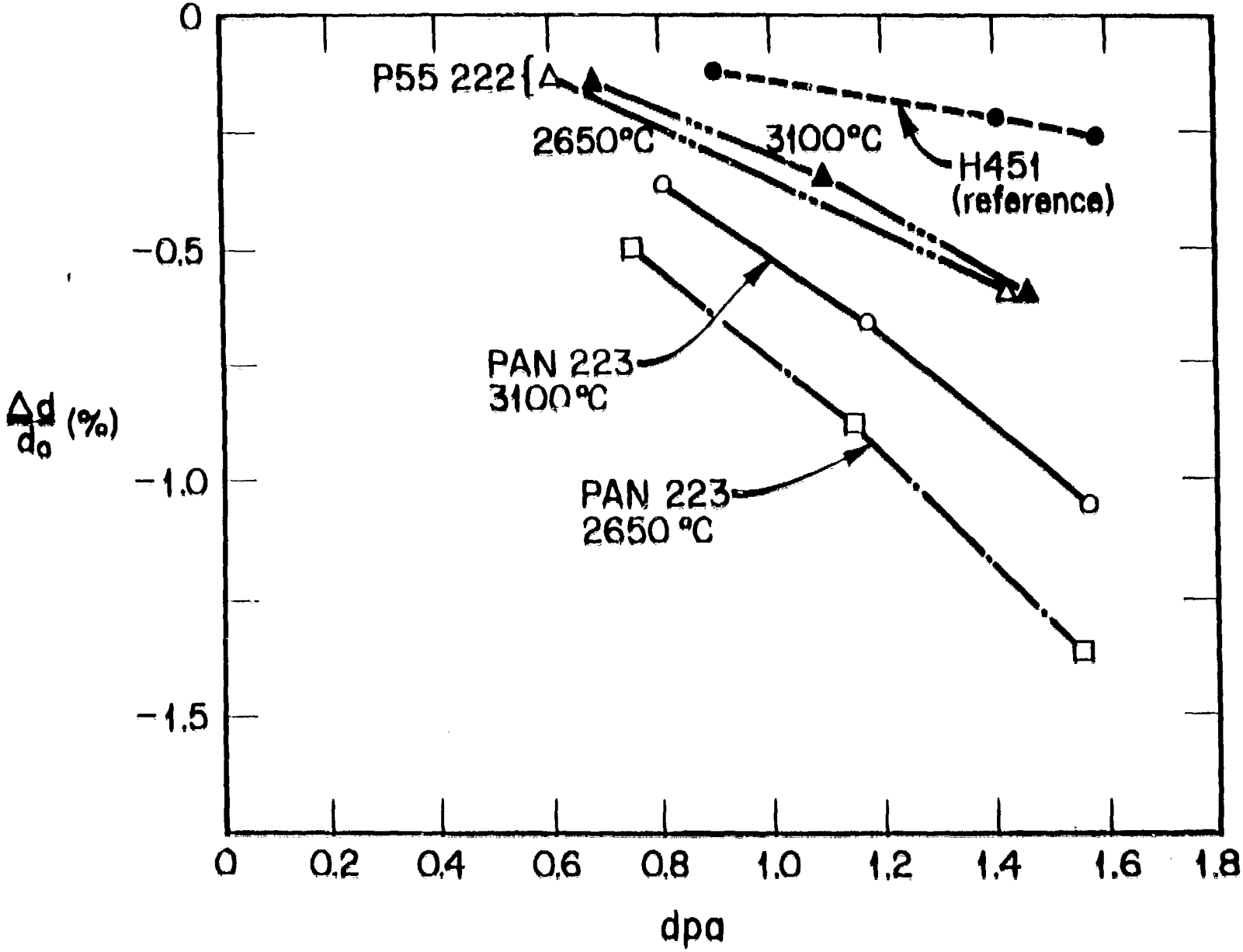
0
-0.5
-1.0
-1.5
$\frac{\Delta d}{d_o}$ (%)
P55 222{
2650°C
3100°C
H451
(reference)
PAN 223
3100°C
PAN 223
2650°C
0
0.2
0.4
0.6
0.8
1.0
1.2
1.4
1.6
1.8
dpa

Fig. 6

ornl

ORNL-DWG 91-11264R

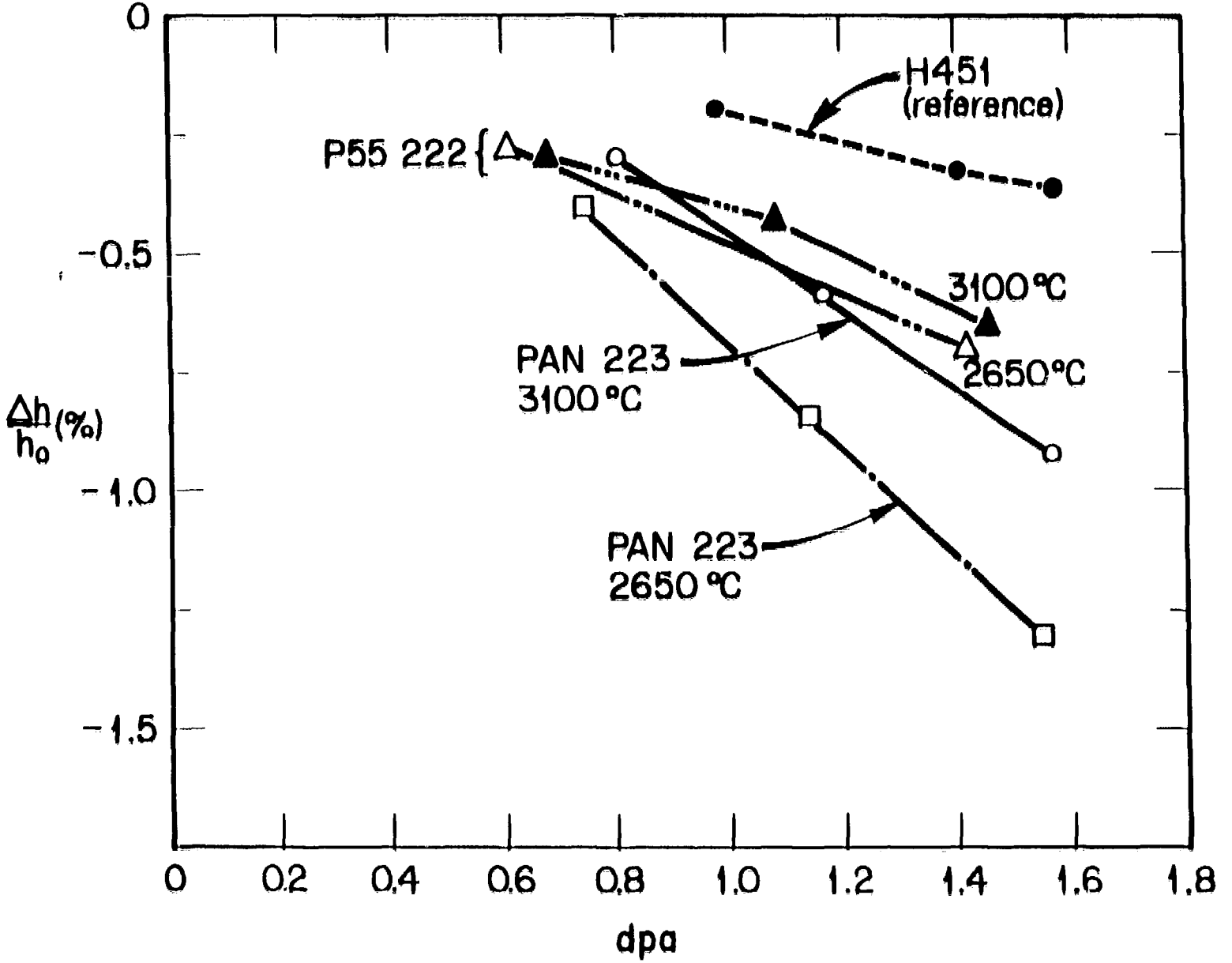

Fig. 7

ornl

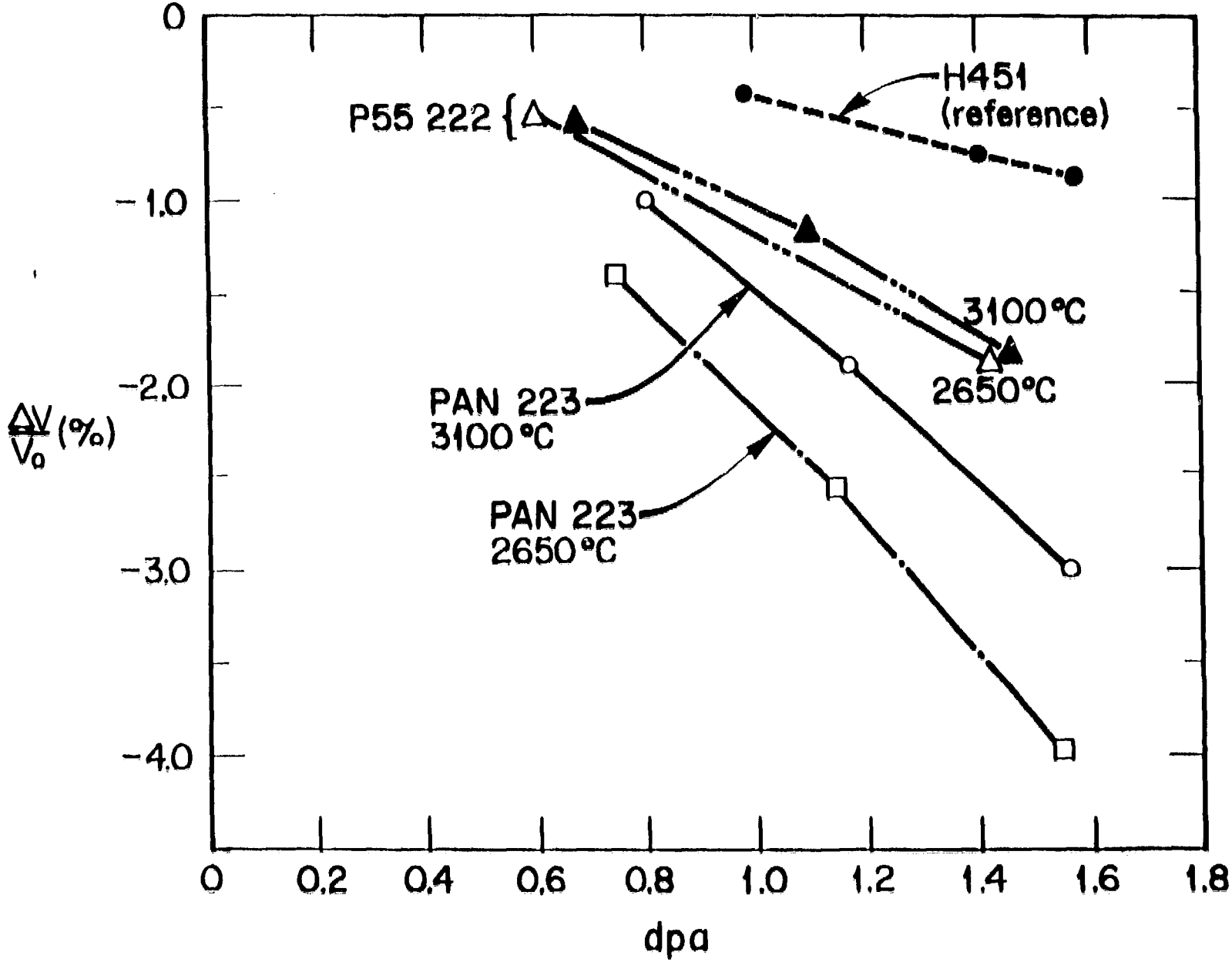
0
-1.0
-2.0
-3.0
-4.0
ΔV/V0 (%)
P55 222
H451
(reference)
3100°C
2650°C
PAN 223
3100°C
PAN 223
2650°C
0
0.2
0.4
0.6
0.8
1.0
1.2
1.4
1.6
1.8
dpa

Fig. 8

ornl

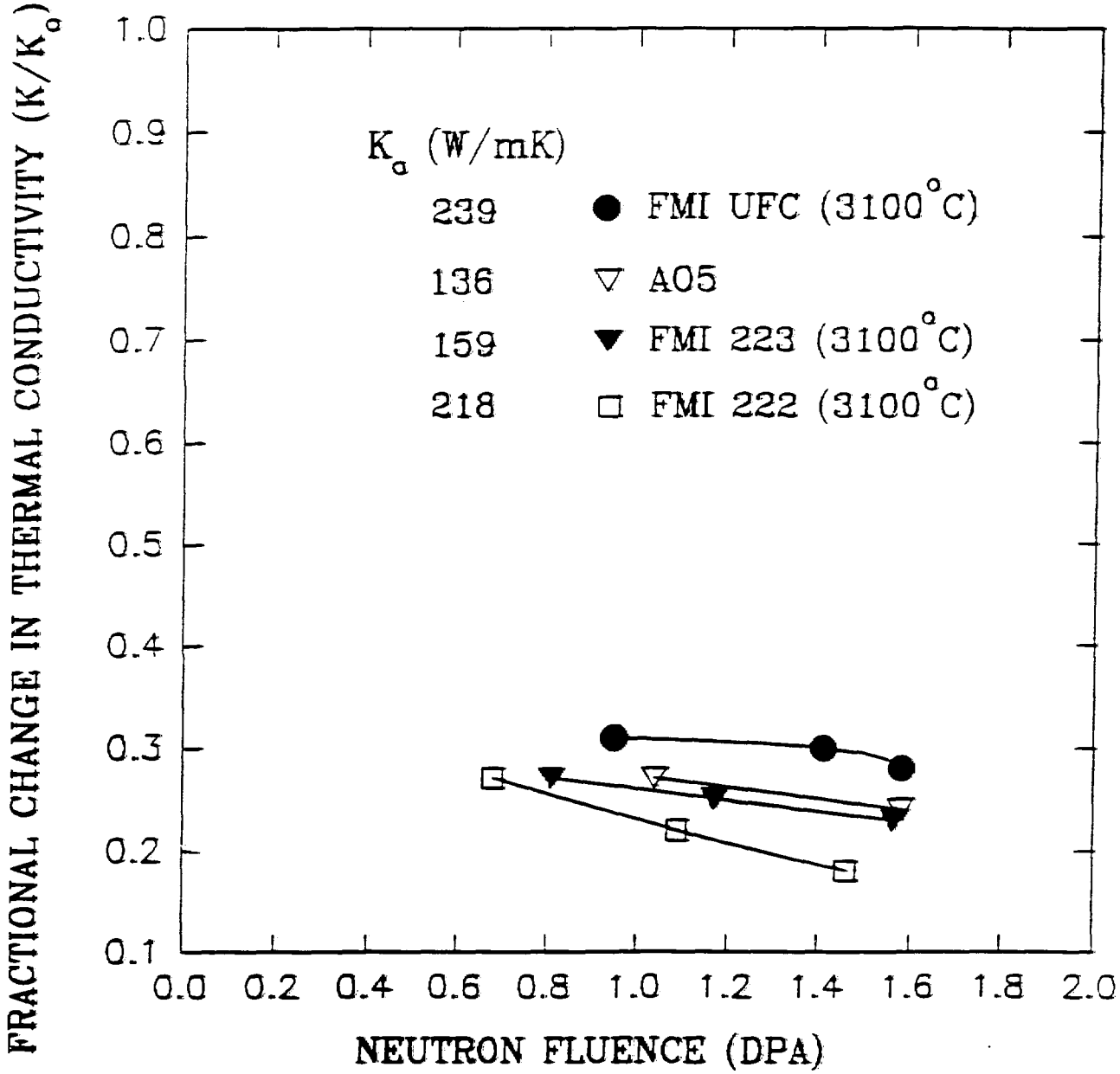
FRACTIONAL CHANGE IN THERMAL CONDUCTIVITY (K/K$_a$)
1.0
0.9
0.8
0.7
0.6
0.5
0.4
0.3
0.2
0.1
K$_a$ (W/mK)
239
136
159
218
FMI UFC (3100°C)
A05
FMI 223 (3100°C)
FMI 222 (3100°C)
0.0
0.2
0.4
0.6
0.8
1.0
1.2
1.4
1.6
1.8
2.0
NEUTRON FLUENCE (DPA)

Fig. 9